

Large Field of View, High Spatial Resolution, Surface Measurements

James C. Wyant and Joanna Schmit
WYKO Corporation, 2650 E. Elvira Road
Tucson, Arizona 85706, USA
jcwyant@wyko.com and jschmit@wyko.com
www.wyko.com

&

Optical Sciences Center
University of Arizona
Tucson, Arizona 85721, USA
www.opt-sci.arizona.edu

SUMMARY

It is difficult in interferometric metrology to maintain high spatial resolution over a large field of view. Interferometric microscope measurements yield high resolution, but only over a small area. Other conventional interferometric systems can measure large areas, but they fail to provide the necessary spatial resolution. High spatial resolution over a large field-of-view (FOV) can be obtained by stitching together multiple high spatial resolution measurements of adjacent areas of a measured surface. The measurements can be fit together in a global sense, or by matching the piston and tilt over the overlap region. Care must be taken in the stitching process to make sure the measurements are precisely overlapped to minimize errors. The larger the overlap the easier it is to match data sets, but of course more data sets are required to get a given field of view. This paper shows that a 20 percent overlap gives a good trade off between having good repeatability and obtaining a large field of view with a minimum number of data sets. Typical measurement results are shown for stitching as many as 285 sub-regions.

1. INTRODUCTION

Interferometric optical microscopic profilers are often used for the measurement of surface microstructure (1-3). Two modes of operation are generally available for the optical profilers. For smooth surfaces the phase-shifting integrating bucket technique is generally used since it gives sub-nanometer height resolution capability (4-5). For rougher surfaces, a vertical scanning coherence sensing technique can be used to give nanometer height resolution over several hundred microns of surface height (6-9).

In order to obtain sufficiently high spatial sampling the FOV is typically very small. As an example, for a commonly used 740 x 480 element detector array and a 1.5X magnification between the sample and the detector array, the spatial sampling is 6.6

microns and the FOV is 4.9 x 3.2 mm. For a 50X magnification, the spatial sampling is 0.2 microns and the FOV is 0.15 x 0.10 mm. One approach for increasing the FOV, while keeping the spatial sampling constant, is to use a larger detector array, however this gives only a factor of about 2 increased field. Another approach, which can give a much larger field of view, is to stitch together several smaller FOV measurements to obtain a larger FOV high spatial resolution image. While the stitching approach is not new, the availability of precision stages with high-accuracy optical encoders, and fast micro-computers having lots of memory makes the stitching approach much more attractive at the present time than it was a few years ago. However, there are still many sources of error that must be considered before one can obtain high resolution, large field-of-view images.

2. ERRORS IN STITCHING MEASUREMENT

As with any interferometric testing technique, a number of error sources degrade the accuracy of the measurement. When stitching together multiple topography maps, limiting the sources of these errors becomes especially important because the errors magnify as multiple measurements are introduced. Therefore, we need to consider the error sources of single measurements, as well as those introduced by the stitching process. In this paper we present a classification of important error sources and an analysis of these errors based on real data.

Single measurement error sources.

The errors of a single optical measurement have been addressed in the literature many times (5, 10, 11). Below is a list of common system systematic and random error sources for a single measurement that employ interferometric techniques using a CCD camera for image registration.

- objective distortion and aberrations
- reference mirror shape
- magnification
- pixel aspect ratio
- errors of the measurement technique
- PZT miscalibration,
- detector nonlinearity
- vibration
- errors due to defocus
- system noise

It is worth noting that slightly off magnification or pixel aspect ratio may not be significant for a single measurement; however, when used with a stitching procedure, either may cause an incorrect stage movement and thus misalignment of data in the xy direction.

Stitching process error sources.

The error sources for the stitching measurement can be divided into three categories: system, data stitching, and sample error sources. The list of major error

sources is given below followed by a short description of each of the error sources.

System error sources:

- camera/stage misalignment
- stage movement resolution

Data stitching error sources:

- overlap area
- number of measurements
- stitching order

Sample error sources:

- sample roughness and structure

In stitching measurements it is important to precisely know the distance the sample is moved between measurements. Optical encoders make it possible to know the sample motion to better than one pixel. It is also important to ensure that the movement of the stage stays parallel to the rows and columns in the pixel array of the CCD camera; this is easily achieved to within one pixel.

After completing a full set of measurements, the results are stitched together to form a large surface area topography. Several error sources arise when these individual sets of data are pieced together. Specifically, we concern ourselves with the influence of the overlap of the measured areas, the number of measurements involved and the order in which the sets of data are stitched together. Obviously, all stitching is done using software.

The measured areas need to overlap in order to adjust the relative tilt and piston of each measurement. We sampled three varying percentages of overlap to determine the optimal size of the shared regions. Greater overlap allows for more accurate fitting, whereas minimal overlap enables fewer measurements to be taken. In addition, as the number of measurements increases so does the error when the data is stitched together. The influence of both the size of the overlap region and the number of measurements is shown in Table 1. Finally,

the order in which the single phase maps are stitched together can make a difference, sometimes introducing a large error if care is not taken in designing the software; we show this in a separate example from the one used to demonstrate the other two data stitching error sources.

A third group of errors we identify is error sources introduced by the sample itself. The roughness and structure of the sample may influence how well two data sets are put together; we demonstrate this testing surface roughness standards.

Overlap, number of measurements, and sample roughness.

In order to analyze the influence of the overlap area, the number of measurements and the sample roughness error sources outlined above, the following set of measurements was taken:

Sixteen adjoining measurements (equaling one set) were taken across a surface array divided into four rows and four columns. Ten complete sets of measurements were taken in order to test the repeatability of the stitching measurement. For each single measurement the phase shifting technique was used. The reference wavefront was subtracted from each measurement to eliminate systematic errors, and the measurement with autofocus was chosen to minimize defocus errors, which become significant at higher magnifications. To analyze the repeatability of the stitched measurement the rms (root mean square) of the difference between the stitched measurements was calculated; their averaged values are presented in Table 1. This measurement was taken for three varying percentages of overlap, 5, 20 and 35 percent. From the RMS values we see that the error for 5 percent of overlap is significantly larger than that for 20 and 35 percent. In order to examine the effect that the number of stitched measurements has on

measurement error, we stitched together 3 x 3 and 2 x 2 measurement arrays from the existing data. For each percentage of overlap regions, the smallest error was achieved for the smallest number of stitched data, and for the largest overlap region the error was the smallest. From the table it is clear that as the overlap region decreases or the number of measurements increases the stitched measurement error gets larger. The 20% overlap region seems to be a good compromise between accuracy and speed.

Table 1: Average values of RMS (nm) of difference between two stitched measurements.

Number of Files	5% overlap	20% overlap	35% overlap
Roughness standard RMS=0.5nm			
16 (4x4 files)	2.69	0.62	0.46
9 (3x3)	1.03	0.44	0.25
4 (2x2)	0.96	0.36	0.26
Roughness standard RMS=1.5nm			
9 (3x3)	1.55	0.54	0.37
4 (2x2)	0.96	0.51	0.34

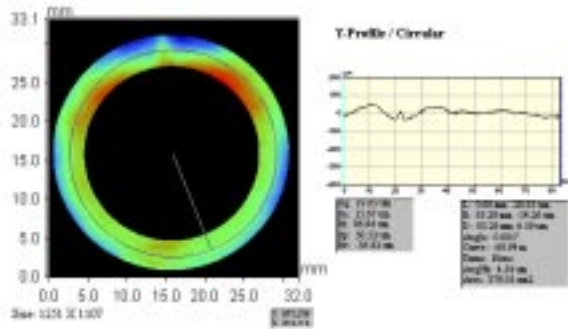
This table also contains values for the measurement of the sample of 1.5nm RMS surface roughness (3x3 and 2x2 measurements). When the RMS difference values are compared with RMS difference values for respective measurements of two samples with different surface roughness, it can be concluded that larger sample roughness will cause larger error in stitched measurement.

Stitching order.

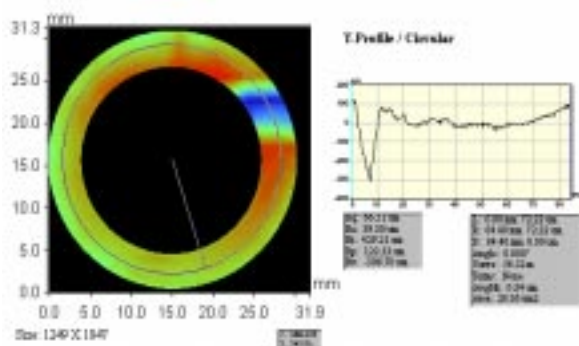
The importance of the order in which measurements are stitched becomes significant when two neighboring measurements have much less than a 20%

overlap of data (see Table 1). This kind of situation may occur when the shape of tested element is not rectangular but rather, for example, is circular. When the circular shape is divided into a grid, the outer-most

areas should be stitched last. Figures 1a and 1b present a stitched measurement of the top surface of a fuel cap. The measurements in Fig.1a were stitched in a good order while in Fig. 1b the measurements were stitched in an order that resulted in a large stitching error. In short then, when testing irregular shaped elements, it is important to pay attention and optimize the stitching order so that any possibility of stitching order error is minimized.



(1a) Correctly stitched measurement



(1b) Incorrectly stitched measurement

Figure 1. Measurement of fuel cap.

cells may not contain much data that overlaps with all neighboring cells. This is because the tested element does not fill the whole field of view. A cell that contains a very small portion of valid data may introduce large errors when it is the first element stitched. In addition, this error may propagate when stitching the rest of data. In order to avoid large stitching errors, cells with large overlaps of valid data should be stitched first and cells with small overlap

Number of stitched measurements

The largest number of measurements that we have stitched so far is 285. This measurement was performed for a magnetic hard disk (see Fig. 2) where high gradients of the surface did not allow for a good measurement with a conventional interferometer. A large number of data points had to be used to resolve the fringes, but since this high density of data points was not needed in the evaluation of the data, in the stitching process only every 4th data point was used. The number of files to be stitched is really limited only by the computer's memory and the user's time.

Comparison of single and stitched measurements.

In order to test the validity of stitched measurements, we compared the results we obtained with the stitching technique using an interference microscope with those gathered with a single measurement from a Fizeau interferometer. In this test we analyzed the surface topography of a flat mirror 20mm in diameter. The stitching procedure employed 48 single measurements. The stitched measurement gave an RMS of 1.79 nm and the mirror tested with the Fizeau gave an RMS of 1.55 nm. Note that in this case the RMS values are a measure of the surface geometry not

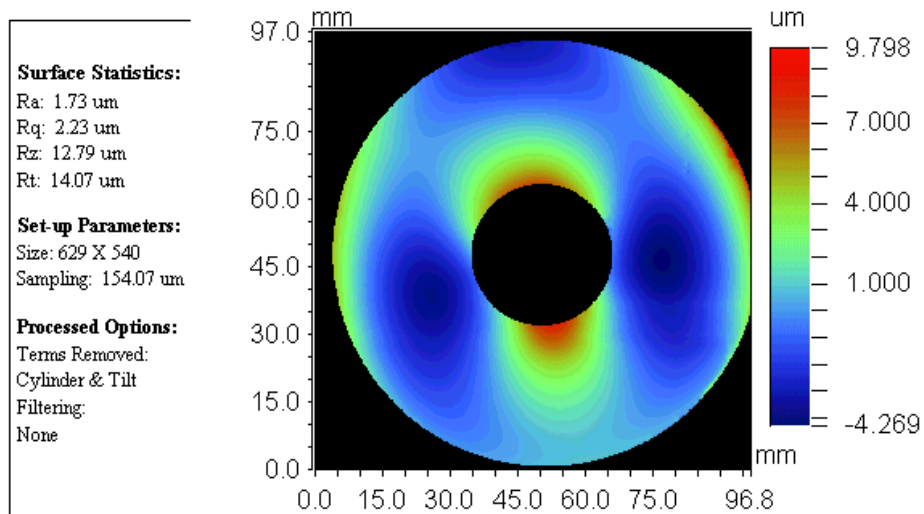


Figure 2. Magnetic hard disk - 285 stitched measurements.

its roughness. It is important to note that in each of the measurements the reference wavefront was subtracted to eliminate the systematic errors of each of the systems. Reference subtraction is very important in stitching measurements to eliminate artifacts introduced by errors in the reference surface.

3. TYPICAL MEASUREMENTS

Hundreds of samples have been measured using the stitching technique and both phase shifting and vertical scanning techniques. Below we will show three typical results.

Figure 3 shows the inside of an engine bore obtained using six stitched data sets. In this case a small interferometric optical microscope was made that fits inside the cylinder so the measurements could be made without damaging the engine bore. Figure 4 shows a picture of the instrument making a measurement. For this measurement a precision stage was not used to obtain the measurements, but rather the surface being measured had enough texture that the separate measurements could be sufficiently

well aligned by looking at the structure in the measured surface contour maps and aligning the overlap regions.

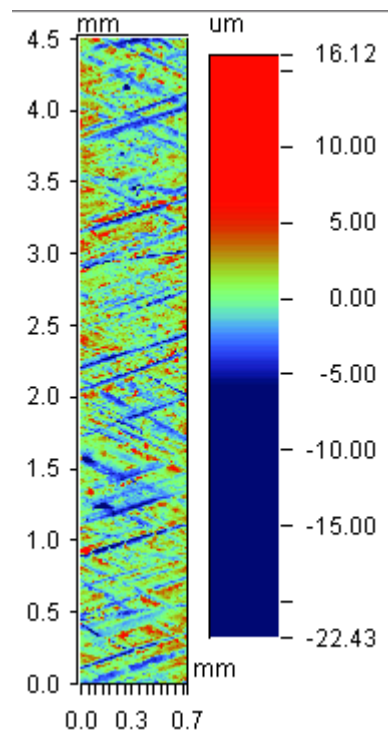


Figure 3. Six stitched data sets showing the inside of an engine cylinder bore. (Ra=1.69 μm , Rq=2.22 μm , Rz=27.87 μm , and Rt=38.54 μm .)

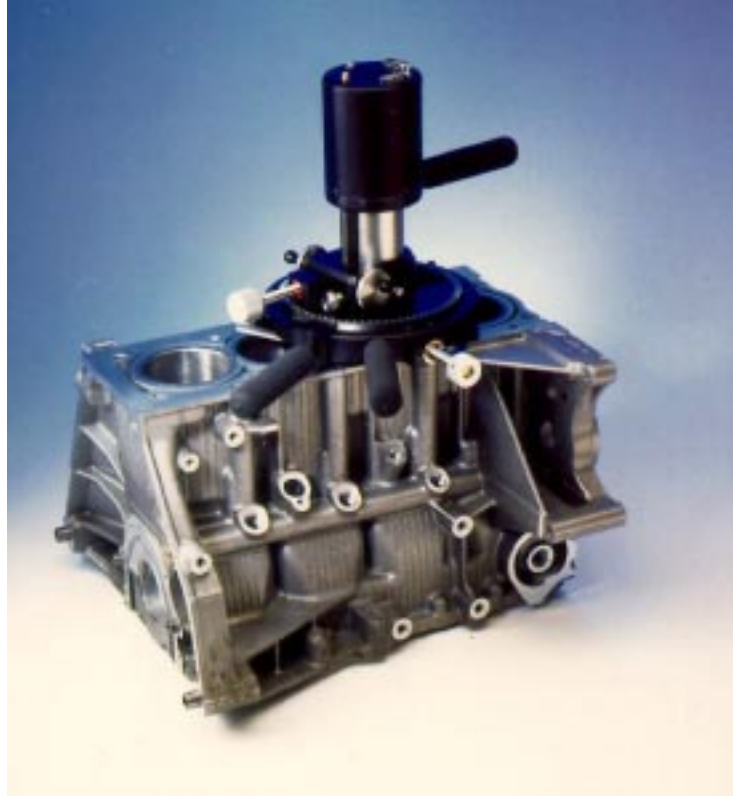


Figure 4. Insight 2000 measuring the inside of an engine bore.

Figure 5 shows results for measuring a valve disk in a diesel engine fuel injector. The critical measurement is the waviness of a circumferential slice at a 2.5 mm radius from the center. Several attempts were made to measure this sample using various commercial flatness measuring interferometers, but the desired spatial resolution could not be obtained because of both an insufficient number of detector pixels, and in most cases poor optical resolution. The measurement was very easy to perform using a microscopic profiler and a 3 x 4 stitched array.

Figure 6 shows the results for measuring a lapping bar for magnetic recording heads. Figure 6a shows the entire lapping bar and

Figure 6b shows in zoomed in portion of the lapping bar. In this case the stitching approach was important for two reasons. First, the bar departed from flatness by so much that thousands of data points along the length of the bar were required to resolve the interference fringes. A normal commercial phase-shifting flatness measuring interferometer could not measure the entire surface of the lapping bar in one measurement. Secondly, the higher frequency structure in the surface shape was of interest. By using the stitching technique it was possible to obtain the overall measurement, and then the data could be zoomed-in to get the high frequency information.

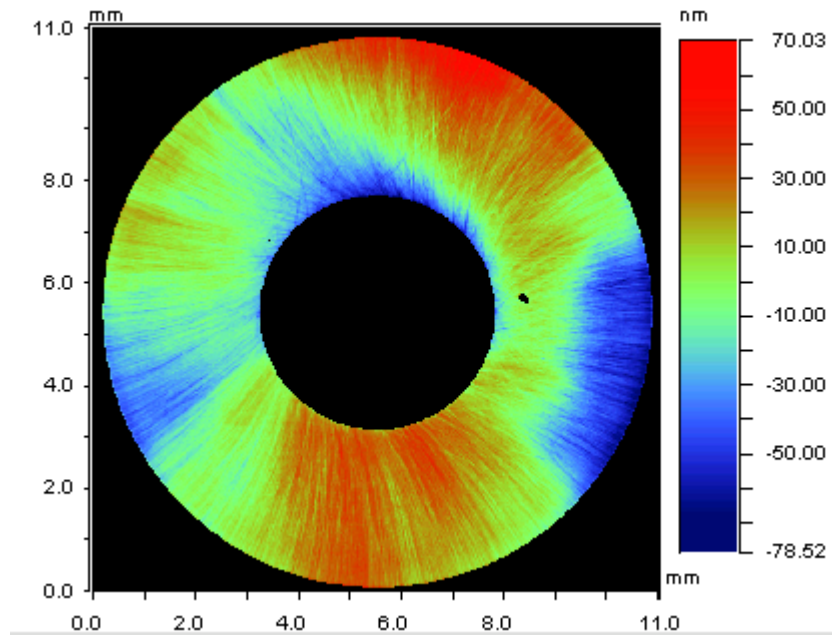
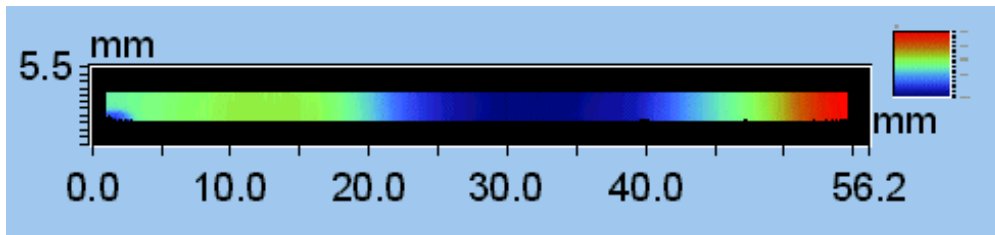
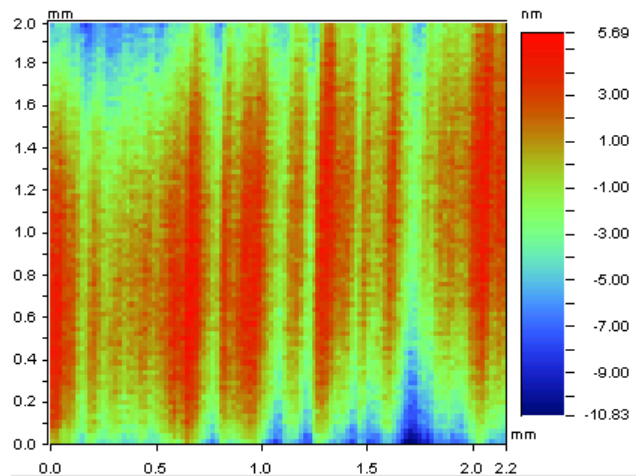


Figure 5. 3 x 4-stitched array made of a diesel engine fuel injector.



a) Entire lapping bar. . 2787 x 236 data points. Ra =413 nm and Rt=1.88 micron.



b) Zoomed-in portion of lapping bar.

Figure 6. Lapping bar for magnetic recording heads

4. CONCLUSIONS

This paper has shown several examples of using stitching techniques to measure a variety of surfaces. As long as the overlap area between adjacent areas is kept to on the order of 20%, and the stitched surfaces are

properly aligned, the loss in accuracy is acceptable. The ability to stitch surfaces to obtain high lateral resolution over a large field of view should further increase the applications of phase-shifting and vertical scanning interferometric profilers.

REFERENCES

1. B. Bhushan, J.C. Wyant and C.L. Koliopoulos, "Measurement of surface topography of magnetic tapes by Mirau interferometry", *Appl. Opt.*, 28:1489-1497, 1985.
2. J.C. Wyant, "Optical profilers for surface roughness", *Proceedings of the Society of Photo-Optical Instrumentation Engineers*, 525, 174-180, 1985.
3. J. C. Wyant and K. Creath, "Advances in Interferometric Optical Profiling," *Int. J. Mach. Tools Manufact.* Vol. 32, No.1/2, 5-10(1992).
4. J. C. Wyant, "Use of an ac heterodyne lateral shear interferometer with real-time wavefront corrections systems," *Appl. Opt.* 14(11): 2622-2626, Nov. 1975.
5. K. Creath, "Phase-Shifting Interferometry Techniques," in *Progress in Optics XXVI*, E. Wolf, ed. (Elsevier Science, 1988), pp. 357-373.
6. M. Davidson, K. Kaufman, I. Mazor, and F. Cohen, "An Application of Interference Microscopy to Integrated Circuit Inspection and Metrology," *Proc. SPIE*, 775, 233-247 (1987).
7. G. S. Kino and S. Chim, "Mirau Correlation Microscope," *Appl. Opt.* 29, 3775-3783 (1990).
8. T. Dresel, G. Hausler, and H. Venzke, "Three-dimensional sensing of rough surfaces by coherence radar," *Appl. Opt.* 31(7): 919-3925, March 1992.
9. P. J. Caber, "An Interferometric Profiler for Rough Surfaces," *Appl. Opt.* 32(19): 3438-3441, July 1993.
10. K. Creath, "Phase-measurement interferometry: beware these errors," *Proc. SPIE* 1553, (1991).
11. J. Schwider, "Advanced evaluation techniques in interferometry," in *Progress in Optics XXVIII*, E. Wolf, ed. (Elsevier, New York, 1990), 271-359.